21. I. Wilkinson, P. Engels, M. D. Houslay, *Pharmacol. Rev. Commun.* **9**, 215 (1997).
22. G. A. Omburo, S. Jacobitz, T. J. Torphy, R. W. Colman, *Cell. Signalling* **10**, 491 (1998).
23. L. S. Beese and T. A. Steitz, *EMBO J.* **10**, 25 (1991).
24. S. L. C. Jin, J. V. Swinnen, M. Conti, *J. Biol. Chem.* **267**, 18929 (1992).
25. I. V. Turko, S. H. Francis, J. D. Corbin, *J. Biol. Chem.* **273**, 6460 (1998).
26. G. P. Livi *et al.*, *Mol. Cell. Biol.* **10**, 2678 (1990).
27. W. J. Rocque *et al.*, *Biochemistry* **36**, 14250 (1997).
28. J. M. Atienza, D. Susanto, C. Huang, A. S. McCarty, J. Colicelli, *J. Biol. Chem.* **274**, 4839 (1999).
29. W. J. Rocque *et al.*, *Protein Expr. Purif.* **9**, 191 (1997).
30. Collaborative Computational Project No. 4, *Acta Crystallogr.* **D50**, 760 (1994).
31. E. De La Fortelle and G. Bricogne, *Methods Enzymol.* **276**, 472 (1997).
32. T. A. Jones, J. Y. Zou, S. W. Cowan, M. Kjeldgaard, *Acta Crystallogr.* **A47**, 110 (1991).
33. A. T. Brünger *et al.*, *Acta Crystallogr.* **D54**, 905 (1998).
34. Candidate syn and anti binding modes of cAMP and cGMP were generated in and around the metal site with Ligand Fit (Cerius2) and also by graphical manipulation. The most plausible binding modes were refined with CHARMm (MSI) or MVP (Glaxo Wellcome) and ranked according to their LUDI (MSI) or MVP scores. ME1 and ME2 were modeled as Zn^{2+} and Mg^{2+}, respectively, and the low-occupancy arsenate ion was omitted.
35. E. Butt *et al.*, *Mol. Pharmacol.* **47**, 340 (1995).
36. Z. Otwinowski and W. Minor, *Methods Enzymol.* **276**, 307 (1997).
37. Coordinates of the PDE4B2B catalytic domain may be obtained from the Protein Data Bank, accession code 1F0J. We thank R. Sweet (NSLS beamline X12C), J. Chrzas (APS beamline 17-ID), Y. Xia and R. Gampe for technical assistance, E. Xu for useful discussions, and P. Jeffs for encouragement and support. Supported by NIH grant AI33072 (H.K.).

7 March 2000; accepted 21 April 2000

Signaling Specificity by Frizzled Receptors in *Drosophila*

Michael Boutros,* Jozsef Mihaly, Tewis Bouwmeester, Marek Mlodzik†

Wnt-Frizzled (Fz) signaling pathways play recurring important roles during the development and homeostasis of vertebrates and invertebrates. Fz receptors can signal through β-catenin–dependent and –independent pathways. In *Drosophila*, Fz and Fz2 are redundant receptors for Wg. In addition, Fz conveys signals through a distinct pathway to organize planar polarization of epithelial structures. We demonstrate that the cytoplasmic sequences of Fz2 and Fz preferentially activate the β-catenin and planar polarity cascade, respectively. Both receptors activate either pathway, but with different efficiencies. Intrinsic differences in signaling efficiency in closely related receptors might be a general mechanism for generating signaling specificity in vivo.

Pattern formation in multicellular organisms relies on specific inductive signaling events. Many evolutionarily conserved signaling pathways are used at multiple times during development to induce tissue- and cell type–specific responses (*1*). Despite the importance of context-dependent signaling specificity, the underlying mechanisms have remained elusive.

Frizzled (Fz) proteins act as receptors for Wnt ligands. Most Wnt-Fz signal transduction pathways involve the posttranslational stabilization of the intracellular protein β-catenin (β-cat/Arm) (*2*, *3*). However, some Fz receptors can also signal through pathways independent of the Wnt–β-cat (Wg-Arm) cascade (*4*–*8*). Both pathways use Dishevelled (Dsh) as a transduction component, raising the intriguing question of how two structurally related receptors signal through a common protein into distinct effector pathways. In *Drosophila*, Fz and Fz2 are redundant receptors for Wg, activating the Wg-Arm cascade (*9*–*13*). Nevertheless, functional differences between Fz and Fz2 in Wg-Arm signaling remain. Fz2 has a higher affinity for Wg than Fz (*12*, *14*), and removal of either Fz or Fz2 has subtle, but different, effects on the patterning of the embryonic nervous system (*9*). Moreover, only Fz is specifically required for epithelial planar polarity by signaling through a Wg-Arm–independent pathway (*4*, *6*, *7*).

Fz overexpression during *Drosophila* eye development (*15*) causes a gain-of-function (GOF) planar polarity phenotype (*4*, *16*). Overexpression of Fz2 in the developing wing activates Wg-Arm targets (*14*, *16*). To compare the functional equivalence of Fz and Fz2 (we will refer to Fz as Fz1) for activating either the planar polarity or Wg-Arm pathways, Fz1 and Fz2 were expressed with tissue-specific enhancers (*17*) in imaginal discs during *Drosophila* development (*18*). Whereas Fz1 overexpression in eye (Fig. 1A) (*4*, *16*) and wing discs (*19*) resulted in planar polarity phenotypes, Fz2 expression led to planar polarity defects with only very low penetrance (<1%) (Fig. 1B). Conversely, overexpression of Fz2 in wing imaginal discs led to formation of ectopic bristles [a *wg* GOF phenotype (*14*, *16*, *19*)], whereas Fz1 overexpression did not affect bristle formation (*16*, *19*). Thus, Fz receptors have distinct signaling abilities in imaginal discs, despite their redundant role for Wg-Arm signaling in loss-of-function (LOF) analysis (*9*–*13*).

To assess Wnt–β-cat signaling in a quantifiable in vitro assay, we injected both receptors into *Xenopus* embryos and analyzed Wnt target induction in animal cap explants (*20*–*23*). In this heterologous assay, Fz2 induced strong activation of the Wnt–β-cat targets Xnr-3 and Siamois (Sia), whereas Fz1 induced a much weaker response (Fig. 1C). Thus, taken together with the imaginal disc phenotypes, Fz2 is a strong activator of Wnt–β-cat signaling, and Fz1 is a potent activator of the planar polarity pathway. However, both receptors retain a low intrinsic potential to cross-activate either pathway.

Differential Dsh localization may determine Fz signaling specificity, whereby Fz1, but not Fz2, can induce recruitment of Dsh to the membrane in *Xenopus* (*6*). At normalized protein levels for Fz1 and Fz2, however, we did not observe differences in their ability to recruit Dsh (Fig. 1D). Titration experiments with Fz1 and Fz2 RNA concentrations showed very similar threshold levels for either receptor in Dsh membrane localization (*24*). Thus, differential Dsh recruitment is unlikely to be the mechanism by which specificity between these Fz receptors is generated.

Fz receptors are serpentine transmembrane proteins composed of an extracellular ligand-sequestering domain (CRD), a seven-pass transmembrane segment, and a COOH-terminal cytosolic tail (*25*, *26*) (Fig. 2). To determine which domains in Fz1 and Fz2 are required for directing signaling into either pathway, we constructed chimeric and truncated receptors (Fig. 2) (*27*). These chimeric proteins were tested for their signaling potential in *Drosophila* imaginal disc development in wings and nota (with *apGal4*) (*28*), eyes (*15*), and legs (*29*) for their ability to induce either GOF Wg-Arm signaling (Figs. 2 and 3) or planar polarity phenotypes (Figs. 2 to 4).

Both Fz1-2 and Fz1-1-2 chimeric proteins activated a Wg-Arm target (Ac) in the wing imaginal disc (Fig. 3B), induced ectopic marginal bristles (Figs. 2 and 3, G to I), and showed *wg*-associated effects in the leg (*29*). However, they had no significant effect on planar polarity signaling in the eye, the wing, or the notum (Figs. 2, 3, G to I, and 4, C and F). Thus, the Wg-Arm signaling outcome corresponded with the presence of the Fz2 cytoplasmic tail. In contrast, GOF planar polarity phenotypes were observed with chimeric Fz2-1 receptors in the wing (Fig. 3K), the notum (*28*), and the eye

European Molecular Biology Laboratory, Developmental Biology Programme, Meyerhofstrasse 1, 69117 Heidelberg, Germany.

*Present address: Harvard Medical School, Department of Genetics, 200 Longwood Avenue, Boston, MA 02115, USA.

†To whom correspondence should be addressed. E-mail: mlodzik@embl-heidelberg.de

(Fig. 4, B and E) (*15*) that were indistinguishable from those caused by Fz1 (Fig. 2A). Both Fz2-1 and Fz2-2-1 showed a (mild) dominant-negative phenotype for Wg-Arm signaling, as judged by a reduction in Ac expression, (partial) absence of marginal bristles and notches in the wing margin (Figs. 2 and 3, C and J), and the presence of stunted legs (*29*). These data suggested that the chimeric receptors containing the high-affinity Fz2 CRD (*14*), but lacking intracellular Fz2 sequences, can sequester Wg efficiently without eliciting an efficient signal transduction response. To test this possibility directly, we analyzed stabilization of Wg in wing discs (*30*). Whereas Fz1 or Fz1-2 type chimeras had no significant effect on Wg stability (Fig. 3L), all chimeric receptors with the Fz2 CRD strongly sequestered Wg (Figs. 2 and 3, M and N) (*30*). The importance of cytoplasmic sequences for efficient Wnt target activation was confirmed in *Xenopus* animal cap assays (exchanging cytoplasmic domains switched the signaling efficiency) (Fig. 2) (*20*). All chimeric receptors were able to recruit Dsh indistinguishably from wild-type Fz1 and Fz2.

The observation that the Fz1-2 chimera did not dominantly interfere with planar polarity signaling in the eye and because as yet no "planar polarity" ligand has been identified raised the question of whether planar polarity signaling depends on the presumed ligand binding Fz1 CRD. We tested this hypothesis by rescue of the *fz-/-* polarity mutant with *sev-Fz1* and chimeric transgenes. In contrast to Fz1, however, neither Fz1-2 and Fz2-1 chimeras nor Fz2 rescued the *fz* mutant (Fig. 2A), indicating that the Fz1 CRD, coupled to its signaling unit, is required for correct levels of activation of planar polarity signaling in the eye in vivo. Thus, although overexpression of Fz2-1 induces a GOF planar polarity phenotype, identical to that induced by Fz1, it cannot replace Fz1 in a LOF background. Although both receptor isoforms, Fz1 and Fz2-1, when overexpressed (*31*) are capable of activating planar polarity signaling and perturbing correct polarity determination, the pathway is activated to the correct level only by the Fz1 CRD (and ligand)–dependent regulation of the receptor. Because the establishment of correct ommatidial polarity results from small differences in Fz signaling levels between neighboring R3 and R4 cells, the ability to precisely respond to the ligand in a spatially and temporally controlled manner is essential (*32*). Presumably, only Fz1 is appropriately regulated through its CRD to instruct correct ommatidial polarity.

Fz1 and Fz2 appear to have different abilities to activate Wg-Arm and planar polarity signaling in the GOF assays in imaginal discs. Whereas Fz2 induces a Wg-Arm GOF phenotype, Fz1 causes GOF planar polarity phenotypes. The chimeric receptors define the respective cytoplasmic tail (Fz2) or the cytoplasmic domains (Fz1) as largely, but not solely, responsible for mediating these differences in the GOF assays. The Wg-Arm GOF phenotype is ligand- and CRD domain–dependent, as it can only be observed close to the source of Wg (Fig. 3). Also, Fz2 has a stronger effect than Fz1-2 or Fz1-1-2. The planar polarity ligand is, possibly, a member of the Wnt family with a different CRD binding affinity from that of Wg. The mechanism by which the ligand-CRD interaction regulates Fz signaling is unclear. The present data cannot distinguish between an activating (conformational) change, or alternatively, a constitutive signaling capacity by Fz's that is inhibited by another factor and needs to be antagonized by the ligand (similar to Smoothened/Patched signaling with Hedgehog).

How can one reconcile the Fz1 and Fz2 redundancy for Wg signaling in LOF analysis

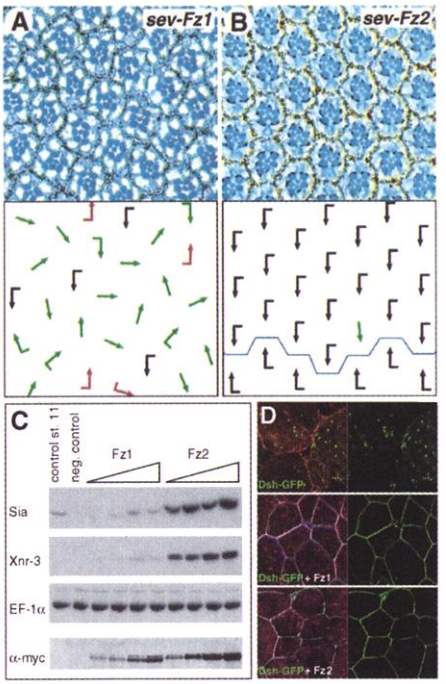

Fig. 1. Frizzled receptors have different intrinsic signaling abilities. Tangential sections of eyes from *sev-Fz1* (**A**) and *sev-Fz2* (**B**) flies (with schematic drawing representing ommatidial orientation). Only Fz1 is effective at inducing planar polarity defects; Fz2 rarely causes planar polarity defects [<1%; only a single symmetrical ommatidium is apparent in the field (green arrow in schematic)]. (**C**) In *Xenopus* animal caps, Fz2 induces the Wnt–β-cat targets Siamois (Sia) and Xnr-3 more efficiently than Fz1. The concentration dependence of induction is readily apparent. Even at the highest Fz1 levels, Wnt target induction is lower than that of low Fz2 levels. Expression of Sia and Xnr-3 was measured by RT-PCR, with EF-1α serving as loading control. All experiments, including those in Fig. 2, were controlled for protein levels, with the myc epitope inserted in the receptors (Fig. 2 legend) or antibodies to Fz1 (*19*). (**D**) Both Fz1 and Fz2 efficiently recruit Dsh to the membrane, indicating that differential subcellular Dsh localization does not determine signaling efficiency and specificity. Dsh is detected as Dsh-EGFP (enhanced green fluorescent protein) (green), and cortical actin is visualized with rhodamin-coupled phalloidin (red). The overlay is shown in white. Dsh-EGFP alone is localized to cytoplasmic structures, but in the presence of either Fz1 or Fz2, completely relocalizes to the membrane.

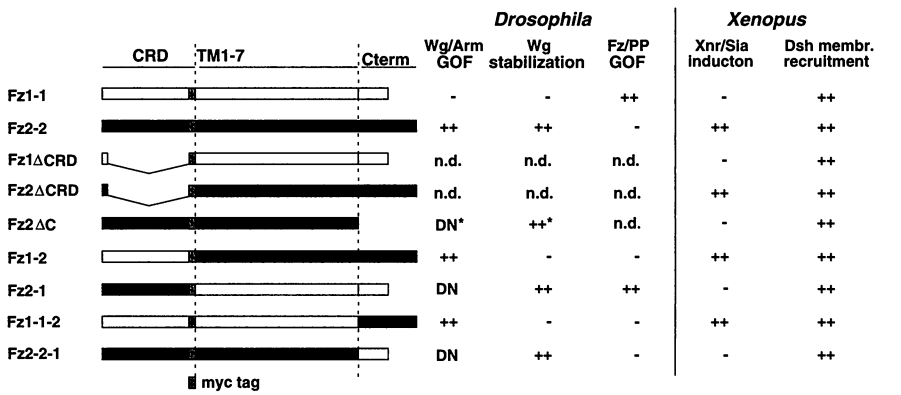

	Drosophila			Xenopus	
	Wg/Arm GOF	Wg stabilization	Fz/PP GOF	Xnr/Sia inducton	Dsh membr. recruitment
Fz1-1	-	-	++	-	++
Fz2-2	++	++	-	++	++
Fz1ΔCRD	n.d.	n.d.	n.d.	-	++
Fz2ΔCRD	n.d.	n.d.	n.d.	++	++
Fz2ΔC	DN*	++*	n.d.	-	++
Fz1-2	++	-	-	++	++
Fz2-1	DN	++	++	-	++
Fz1-1-2	++	-	-	++	++
Fz2-2-1	DN	++	-	-	++

Fig. 2. Mapping the Fz1/2 domain signaling requirements. Schematic representation of the chimeric receptor constructs used in this study. Fz1 parts are indicated as white boxes, and Fz2 parts as black boxes (the inserted myc epitope tag is indicated in gray). The receptors were subdivided into their three major regions: the ligand binding extracellular CRD, the seven-pass transmembrane region, and the cytoplasmic tail. The behavior of the chimeric and truncated receptors was analyzed in *Drosophila* for GOF Wg-Arm and planar polarity effects as well as Wg stabilization, and in *Xenopus* for Xnr-3/Sia induction (see Fig. 1C for examples). The ability of the chimeras to efficiently induce Wg-Arm (*Drosophila*) or Wnt–β-cat (*Xenopus*) signaling correlated with the presence of the cytoplasmic tail of Fz2. All receptor isoforms were membrane anchored, and they induced Dsh membrane localization. (++) Wg-Arm and Fz/planar polarity (PP) signaling (GOF effects in vivo) and Wg stabilization, or efficient Wnt–β-cat target activation and Dsh recruitment to the membrane; (−) very low intrinsic capability of Wnt–β-cat or Fz/planar polarity signaling. DN, dominant-negative behavior for Wg-Arm signaling as judged by the reduction or absence of structures requiring high Wg signaling levels in wings (Fig. 3) and legs (*29*). (*) The equivalent construct for Fz2ΔC in the *Drosophila* experiments was Fz2GPI; n.d., not determined.

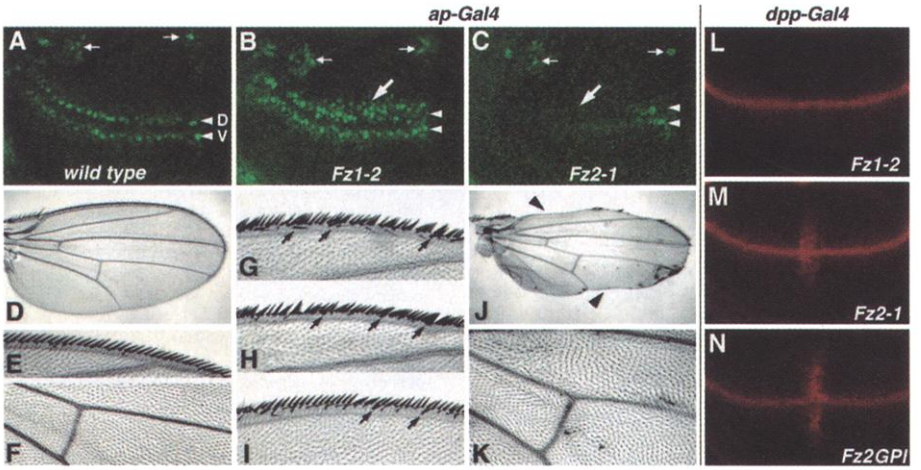

Fig. 3. Specificity of chimeric receptors for Wg signaling in the wing. (**A** to **C**) Confocal analysis of wing discs stained for Achaete (Ac) expression (*37*). Anterior is left and dorsal up. (A) Wild type, (B) *apGal4>Fz1-2*, and (C) *apGal4>Fz2-1* (see Fig. 2 for constructs). In the wild type (A), Wg signaling induces a row of Ac-positive cells (precursors of the wing margin bristles) on either side of the dorsoventral margin (indicated by arrowheads next to "D" and "V"). *wg* is expressed between the two Ac-positive rows at the D/V margin. Other, Wg-independent, Ac-positive cell clusters are indicated with arrows. Overexpression of Fz1-2 (B) leads to the induction of additional ectopic, Ac-positive cells in a Wg-dependent manner, because these cells are only present close to the Wg source near the D/V margin. Overexpression of Fz2-1 (C) leads to a loss of Ac-expressing cells, indicating that high-level Wg signaling is inefficient (*38*). (**D** to **K**) Adult wings: (D to F) Wild type. (E) Higher magnification of the anterior margin with the Wg-dependent sensory bristles; (F) higher magnification of wing blade area illustrating regular arrangement of wing-cell hairs and polarity. (G to I) *apGal4>Fz1-2*. Overexpression of either Fz2 (*19*) or the Fz1-2 chimeras leads to generally malformed, often unfolded wings. The anterior margin in these malformed wings shows the presence of additional ectopic bristles on the dorsal surface, near the margin [indicated by arrows; compare with (E) for the wild type]. The polarity appears normal. (J and K) *apGal4>Fz2-1*. Overexpression of Fz2-1 leads to a (partial) loss of the wing margin (arrowheads), in accordance with a reduction of Ac expression (C). Planar polarity is also affected [(K); compare with (F) for the wild type] similarly to Fz1 (*16*). *ap* is expressed only in the dorsal wing, and polarity defects are accordingly restricted to the dorsal surface. The loss of wing-margin tissue with Fz2-1 and Fz2-2-1 appears to be partially nonautonomous, possibly by serving as a sink for Wg and reducing the availability of Wg on either side. About 30% of the wings displayed a phenotype as shown in (J); the other wings displayed a slightly weaker phenotype, but all wings of these genotypes showed some margin loss. (**L** to **N**) Wing discs of *dppGAL4*-driven Fz1-2 (L), Fz2-1 (M), and Fz2GPI (N) and stained for Wg. Chimeric and truncated receptors with the Fz2 CRD caused Wg stabilization in the *dpp* expression domain, perpendicular to normal *wg* expression along the D/V boundary. Fz1-2 behaved like the wild type. For a summary, see Fig. 2.

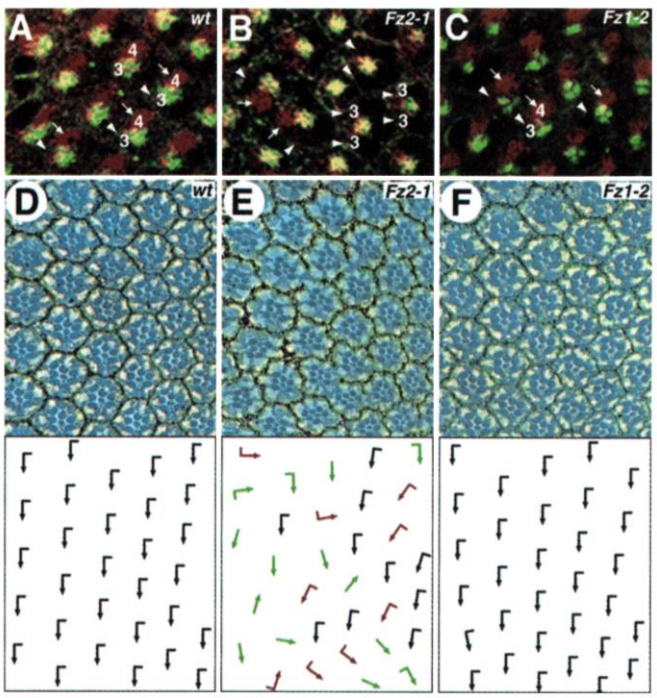

Fig. 4. Specificity of chimeric receptors in planar polarity signaling in the eye. (**A** to **C**) Confocal analysis of eye discs stained for the R4-specific marker H123 (*15*) (red), and fluorescein isothiocyanate–phalloidin (green) highlighting the center of each ommatidial precluster. (A) Wild type, (B) *sev-Fz2-1*, and (C) *sev-Fz1-2* (see Fig. 2 for constructs). In the wild type (A), the R4 cell expresses H123 (arrows), whereas R3 shows only very weak staining (arrowheads). A similar pattern is seen for *sev-Fz1-2* (C). *sev-Fz2-1* shows a typical GOF polarity eye phenotype, with many clusters displaying R3/R3 pair ommatidia (visible by very low or no H123 expression; arrowheads) or randomized R3/R4 distribution within clusters. (**D** to **F**) Tangential sections of eyes from the indicated genotypes with schematic drawing. *sev-Fz2-1* causes phenotypes that are indistinguishable from Fz1 (Fig. 1A).

(*13*) and the dominant-negative behavior of the Fz2-1 chimeras? Fz2 is a high-affinity Wg receptor (*14*) (Fig. 3), and *fz2* transcription is down-regulated by Wg, whereas Fz1 (a low-affinity receptor) is expressed fairly uniformly. Thus, Fz2 might be the primary Wg receptor, and Fz1 substitutes only in its absence. Moreover, another *Drosophila* Fz family member, Fz3, acts as a negative attenuator of Wg signaling and is positively regulated by Wg (*33*), suggesting that the expression patterns of Fz2 and Fz3 shape the Wg response, whereas Fz1 does not contribute to this effect. In this context, overexpression of Fz2-1, consisting of a high-affinity Wg-binding CRD fused to a low-efficiency signaling unit, adversely affects the signaling outcome and causes a dominant-negative phenotype (*34*).

Our experiments provide a model for how signaling specificity can be achieved by closely related receptors, and they demonstrate that LOF studies, like GOF experiments, might only provide a partial answer in case of redundancies. Quantitative differences in ligand affinity and signal transduction efficiency of Fz receptors could provide overlapping and nonoverlapping functions in different cells, depending on the threshold needed to induce targets and expression levels of the various members of the receptor family. Thus, the relative ratio of the different Fz receptors on the cell surface and their degree of occupancy could be an important factor determining the signaling outcome. Additional factors such as coreceptors could influence the signaling outcome, e.g., the heparan sulfate proteoglycan Dally has been identified as a coreceptor in Wg signaling (*35*, *36*). Fz1 and Fz2 signaling preferences provide an example of how quantitative differences in signaling levels can lead to redundant and specific roles of these receptors during development and evolution.

References and Notes

1. P. O. Hackel, E. Zwick, N. Prenzel, A. Ullrich, *Curr. Opin. Cell Biol.* **11**, 184 (1999).
2. K. M. Cadigan and R. Nusse, *Genes Dev.* **11**, 3286 (1997).
3. R. T. Cox and M. Peifer, *Curr. Biol.* **8**, 140 (1998).
4. D. I. Strutt, U. Weber, M. Mlodzik, *Nature* **387**, 292 (1997).

5. M. Kengaku *et al.*, *Science* **280**, 1274 (1998).
6. J. D. Axelrod, J. R. Miller, J. M. Shulman, R. T. Moon, N. Perrimon, *Genes Dev.* **12**, 2610 (1998).
7. M. Boutros, N. Paricio, D. I. Strutt, M. Mlodzik, *Cell* **94**, 109 (1998).
8. L. C. Sheldahl, M. Park, C. C. Malbon, R. T. Moon, *Curr. Biol.* **9**, 695 (1999).
9. K. M. Bhat, *Cell* **95**, 1027 (1998).
10. J. R. Kennerdell and R. W. Carthew, *Cell* **95**, 1017 (1998).
11. H. Mueller, R. Samanta, E. Wieschaus, *Development* **126**, 577 (1999).
12. P. Bhanot *et al.*, *Development* **126**, 4175 (1999).
13. C.-N. Chen and G. Struhl, *Development* **126**, 5441 (1999).
14. K. M. Cadigan, M. P. Fish, E. J. Rulifson, R. Nusse, *Cell* **93**, 767 (1998).
15. Fz1, Fz2, and the chimeric receptors were expressed with *sevGal4* in the developing eye, in a specific subset of photoreceptor precursors (in R3 and R4 at the time of polarity determination). For analysis in imaginal discs, the enhancer trap line H123 was used as a marker for R4 and detected as described [M. Fanto and M. Mlodzik, *Nature* **397**, 523 (1999)]. Eye imaginal discs and sections of adult eyes were prepared, photographed, and processed as described [D. I. Strutt, U. Weber, M. Mlodzik, *Nature* **387**, 292 (1997)].
16. J. Zhang and R. W. Carthew, *Development* **125**, 3075 (1998).
17. A. H. Brand and N. Perrimon, *Development* **118**, 401 (1993).
18. Several independent lines were generated for these and the chimeric constructs, and at least four were tested in the functional assays, all giving equivalent results. The transgenic strains showed comparable protein expression levels as determined by Western blotting with the inserted myc-epitope tag.
19. M. Boutros, J. Mihaly, M. Mlodzik, unpublished results.
20. Capped synthetic RNA of the different receptors was injected into both blastomeres of the two-cell embryo. At stage 9, animal cap ectoderm was explanted and cultured until sibling embryos reached stage 11. Reverse transcriptase–polymerase chain reaction (RT-PCR) was done as described [T. Bouwmeester, S.-H. Kim, Y. Sasai, B. Lu, E. De Robertis, *Nature* **382**, 595 (1996)]. Protein levels were checked by Western blot analysis with anti-myc and anti-Fz1 antibodies. Dsh relocalization assays were done as described [J. D. Axelrod, J. R. Miller, J. M. Shulman, R. T. Moon, N. Perrimon, *Genes Dev.* **12**, 2610 (1998)]. For Xnr-3 and Sia induction, 100 to 800 pg of RNA was injected; for Dsh relocalization, Fz receptors were injected at 100 to 200 pg of RNA together with 100 pg of Dsh-EGFP RNA.
21. M. Brannon and D. Kimelman, *Dev. Biol.* **180**, 344 (1996).
22. F. Fagotto, K. Guger, B. M. Gumbiner, *Development* **124**, 453 (1997).
23. K. Itoh and S. Sokol, *Mech. Dev.* **61**, 113 (1997).
24. Both Fz1 and Fz2 recruited Dsh to the membrane at a concentration of 25 pg of injected RNA and were unable to do so at 12.5 pg, indicating that both receptors have the same threshold in this assay.
25. C. R. Vinson, S. Conover, P. N. Adler, *Nature* **338**, 263 (1989).
26. P. Bhanot *et al.*, *Nature* **382**, 225 (1996).
27. We generated Fz1 and Fz2 chimeric constructs by assembling their CRD (Fz1, amino acids 1 to 166; Fz2, 1 to 219), seven-pass transmembrane region (Fz1, amino acids 167 to 557; Fz2, 220 to 617), and cytoplasmic tails (Fz1, amino acids 558 to 585; Fz2, 618 to 694). In brief, chimeric receptors consisted of 10 base pairs of the Fz1 5′-untranslated region, the CRD domain (except for ΔCRD) linked to the transmembrane region (inserted by generating a Hind III site), and a myc tag in a nonconserved region. For COOH-terminal swaps, a Xho I site was created after the last transmembrane domain. We created chimeric receptors by assembling different fragments in pBS-SK and then shuttling them into *Drosophila* and *Xenopus* expression vectors. Constructs were confirmed by sequencing. For each construct, several independent transgenic *Drosophila* lines were generated and tested in the assays described.
28. The chimeric receptors were expressed under the control of the *apGal4* driver in the dorsal wing and notum. The chimeras that showed mild dominant-negative behavior did not affect *wg* expression at the dorsal/ventral (D/V) margin, indicating that the observed effect is due to Wg read-out defects in the third larval instar. Planar polarity was analyzed in the wing cell hairs (Fig. 3) and by the orientation of the microchaetae on the notum. Effects on planar polarity in the notum were seen with Fz1 and Fz2-1, as is the case in the eye and wing.
29. To analyze the effects of the chimeric receptors in the legs, we used *DllGal4* as a driver (other Gal4 drivers resulted either in all chimeras having a wild-type appearance irrespective of the Fz receptors expressed or were lethal). *DllGal4>Fz1* gave no detectable planar polarity phenotype, whereas *DllGal4>Fz2* was lethal. Fz2-1 and Fz2-2-1 were pupal lethal, showing loss of distal leg structures, a dominant-negative Wg-related effect. Fz1-2 and Fz1-1-2 showed a mild Wg GOF phenotype, as judged by loss of the dorsally derived claws (indicating a transformation to ventral Wg-induced structures) [W. J. Brook and S. M. Cohen, *Science* **273**, 1373 (1996)].
30. To determine the affinity of the different Fz chimeras for Wg, we expressed them with a *dppGal4* driver perpendicular to the normal *wg* expression. All chimeras containing the Fz2 CRD behaved like Fz2 or Fz2CRD-GPI [K. M. Cadigan, M. P. Fish, E. J. Rulifson, R. Nusse, *Cell* **93**, 767 (1998)], leading to Wg stabilization (Fig. 3). The inverse chimeric receptors with the Fz1 CRD had no effect on Wg stability.
31. The Fz1- and Fz2-1–induced GOF planar polarity eye phenotype depends on the amount of Fz expressed in the R3 and R4 precursor cells. At high expression levels (as with Gal4-driven expression), the phenotype is the same in wild-type and in $fz^{-/-}$ eye discs. At lower overexpression levels, the presence of the endogenous protein is important for the overall amounts to reach the threshold necessary for constitutive activation.
32. A small difference in Fz signaling levels between the neighboring R3 and R4 cells is critical to establish correct ommatidial polarity and leads reproducibly to correct polarity; the small difference is amplified by Delta/Notch signaling [M. Fanto and M. Mlodzik, *Nature* **397**, 523 (1999); M. T. Cooper and S. J. Bray, *Nature* **397**, 526 (1999); A. Tomlinson and G. Struhl, *Development* **126**, 5725 (1999)]. The rescue experiments demonstrate that the CRD of Fz1 and a putative ligand are important to establish this difference. Fz2-1 cannot respond to the ligand and establish this difference. Nevertheless, for constitutive activation of downstream pathways the Fz1 CRD is not required.
33. A. Sato, T. Kojima, K. Ui-Tei, Y. Miyata, K. Saigo, *Development* **126**, 4421 (1999).
34. Different signaling preferences of Fz1 and Fz2 are also corroborated by the observation that simultaneous overexpression of Wg and Fz1 in the wing disc neutralizes the GOF effects of each on either Wg signaling or the planar polarity pathway [J. D. Axelrod, J. R. Miller, J. M. Shulman, R. T. Moon, N. Perrimon, *Genes Dev.* **12**, 2610 (1998)].
35. X. Lin and N. Perrimon, *Nature* **400**, 281 (1999).
36. M. Tsuda *et al.*, *Nature* **400**, 276 (1999).
37. S. Romani, S. Campuzano, E. R. Macagno, J. Modolell, *Genes Dev.* **3**, 997 (1989).
38. Wing imaginal discs were dissected from larvae and stained by standard methods. The discs were incubated with mouse antibody to Ac (1:200 dilution; gift of S. Carroll) or to Wg (gift of S. Cohen). Fluorescent-labeled secondary antibody mix (1:500 dilution).

39. We are grateful to P. Adler, K. Basler, S. Carroll, R. Carthew, S. Cohen, R. Nusse, and M. Strigini for fly strains and reagents. We thank members of the Bouwmeester and Mlodzik labs and M. Strigini and S. Cohen for discussions, and J. Curtiss for helpful comments on the manuscript. M.B. was supported by a predoctoral fellowship from the Boehringer Ingelheim Fonds, J.M. is a recipient of a long-term fellowship from the European Molecular Biology Organization.

14 December 1999; accepted 5 May 2000

Economic Incentives for Rain Forest Conservation Across Scales

C. Kremen,[1]* J. O. Niles,[1] M. G. Dalton,[2] G. C. Daily,[1] P. R. Ehrlich,[1] J. P. Fay,[1] D. Grewal,[3] R. P. Guillery[4]

Globally, tropical deforestation releases 20 to 30% of anthropogenic greenhouse gases. Conserving forests could reduce emissions, but the cost-effectiveness of this mechanism for mitigation depends on the associated opportunity costs. We estimated these costs from local, national, and global perspectives using a case study from Madagascar. Conservation generated significant benefits over logging and agriculture locally and globally. Nationally, however, financial benefits from industrial logging were larger than conservation benefits. Such differing economic signals across scales may exacerbate tropical deforestation. The Kyoto Protocol could potentially overcome this obstacle to conservation by creating markets for protection of tropical forests to mitigate climate change.

Each year, an estimated 13 million hectares of forests are destroyed (*1*), 5.6 to 8.6 Gt of carbon are emitted (*2*), and 14,000 to 40,000 species disappear from tropical forests (*3*). Greenhouse gas emissions are likely to increase Earth's temperature by 1° to 4°C in the next century, leading to the possibility of increasingly severe droughts and floods, enhanced rates of species invasion and extinction (*4*), and thus significant economic harm. Tropical deforestation alone is responsible for 20 to 30% of carbon emissions (*5*) and most species extinction worldwide (*6*). Conserving tropical forests could therefore reduce both global warming and biodiversity loss (*7*). Despite conservation efforts, many "protected areas" in the tropics continue to be degraded, while unprotected forests are being converted by logging and agriculture (*8*). We analyzed the economic benefits of forest con-